

Quantum anomalous Hall crystals in moiré bands with higher Chern number

Raul Perea-Causin,^{1,*} Hui Liu,^{1,†} and Emil J. Bergholtz^{1,‡}

¹*Department of Physics, Stockholm University, AlbaNova University Center, 106 91 Stockholm, Sweden*

(Dated: December 5, 2024)

The realization of fractional Chern insulators in moiré materials has sparked the search for further novel phases of matter in this platform. In particular, recent works have demonstrated the possibility of realizing quantum anomalous Hall crystals (QAHCs), which combine the zero-field quantum Hall effect with spontaneously broken translation symmetry. Here, we employ exact diagonalization to demonstrate the existence of stable QAHCs arising from $\frac{2}{3}$ -filled moiré bands with Chern number $C = 2$. Our calculations show that these topological crystals, which are characterized by a quantized Hall conductivity of 1 and a tripled unit cell, are robust in an ideal model of twisted bilayer-trilayer graphene—providing a novel explanation for experimental observations in this heterostructure. Furthermore, we predict that the QAHC remains robust in a realistic model of twisted double bilayer graphene and, in addition, we provide a range of optimal tuning parameters, namely twist angle and electric field, for experimentally realizing this phase. Overall, our work demonstrates the stability of QAHCs at odd-denominator filling of $C = 2$ bands, provides specific guidelines for future experiments, and establishes chiral multilayer graphene as a theoretical platform for studying topological phases beyond the Landau level paradigm.

INTRODUCTION

The rise of moiré materials in the last years has boosted the study of phases with intertwined many-body correlations and topology [1–3]. Concretely, fractional Chern insulators (FCIs)—lattice systems that exhibit the fractional quantum anomalous Hall effect due to spontaneous breaking of time-reversal symmetry [4–15]—were predicted [16–22] and later realized [23–28] in a series of moiré heterostructures based on either graphene or transition metal dichalcogenides. The demonstration of FCI phases in moiré superlattices generated widespread excitement over the possibility of achieving quantized Hall conductance, dissipationless edge currents, and anyonic excitations in an experimentally accessible and highly-tunable platform without the need for a magnetic field. More recently, most efforts have been directed into exploring phases that go beyond the conventional Laughlin and hierarchy fractional quantum Hall (FQH) states. On the one hand, many theoretical works [29–36] have proposed that FCI analogs to non-Abelian FQH states can be stabilized at moiré fractional fillings $\nu = \frac{1}{2}$ [29–35], as well as $\nu = \frac{3}{5}, \frac{2}{5}$ [36], with experimental signatures suggested to correspond to the former [37]. On the other hand, a few works have recovered the concept of quantum Hall crystal [38]—where the topology associated with the quantum Hall effect is accompanied by translation symmetry breaking—and predicted its emergence in different van der Waals heterostructures at zero magnetic field, therefore acquiring the name of quantum *anomalous* Hall crystals (QAHCs) [39–45].

Recent theoretical studies have demonstrated the possibility of realizing QAHCs that are topological analogs of Wigner and generalized Wigner crystals, which break either the continuous translation symmetry in a system with weak or absent moiré modulation [41, 46] or the discrete translation symmetry in a moiré lattice [40]. In the case of the former, the Hall

conductivity maintains an integer value at an extended continuous range of filling factors where the crystal remains stable. In contrast, the moiré QAHC is only stable at the filling factors where a charge density wave (CDW) commensurate with the underlying moiré lattice can form and, importantly, this results in a clear mismatch between the (integer) Hall conductivity and the filling factor. Such fingerprints have been recently found in experiments performed on multilayer graphene systems [47–49]. However, despite the fact that the QAHC presumably observed in bilayer-trilayer graphene might arise from a flat band with Chern number $C = 2$ [48], previous theoretical works have been restricted to $C = 1$ bands. The stability of QAHCs arising from higher Chern bands is an important question that goes beyond the paradigm of traditional quantum Hall and Landau level physics [50–52]. Moreover, apart from moiré-less QAHCs, numerical studies have so far only explored moiré QAHCs at even-denominator filling, while experimental findings also point towards the existence of QAHCs at odd-denominator filling where this phase competes with FCIs and trivial CDWs.

In this work, we investigate the emergence of QAHCs in moiré bands with higher Chern number at odd-denominator filling factor, concretely $\nu = \frac{2}{3}$, by employing exact diagonalization (ED) of the many-body Hamiltonian. First, we consider ideal topological bands in the chiral model of twisted multilayer graphene [53, 54]. Based on the degeneracy and Chern number of the many-body ground state as well as structure factor, pair-correlation function, and hole entanglement spectrum, we identify FCI, QAHC, and compressible liquid phases at $\frac{2}{3}$ filling of ideal $C = 1$, $C = 2$, and $C > 2$ moiré bands, respectively. In particular, the QAHC arising from the $C = 2$ band in the chiral model of twisted bilayer-trilayer graphene is characterized by an average many-body Chern number $C_{\text{avg}} = 1$, consistent with the experimental observations in this material [48], and a K-point CDW modula-

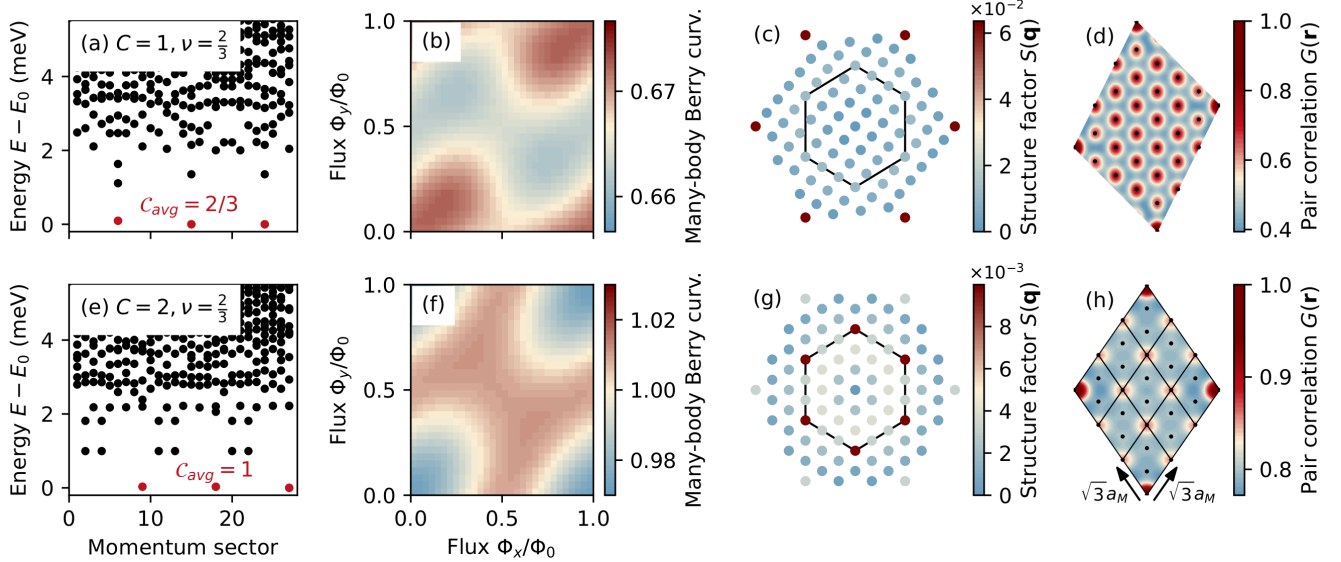


FIG. 1. (a) Many-body energy spectrum, (b) average Berry curvature, (c) structure factor, and (d) pair-correlation function demonstrating the FCI phase at $\nu = \frac{2}{3}$ filling of the ideal $C = 1$ band in a system with $N_s = 27$ sites and generating vectors $\mathbf{R}_1 = (6, 3)$, $\mathbf{R}_2 = (1, 5)$. (e)-(h) are the respective results for the ideal $C = 2$ band demonstrating an integer Hall crystal phase. In the latter case the generating vectors are $\mathbf{R}_1 = (6, 3)$, $\mathbf{R}_2 = (3, 6)$. The Berry curvature $\Omega(\mathbf{k})$ is normalized by the number of flux points $N_\Phi = 30^2$, i.e. $\Omega(\mathbf{k})N_\Phi/2\pi$ is shown here so that the Chern number can be read off directly. The black dots in (d) and (h) denote moiré lattice sites, and the black lines in (h) mark the unit cells of the Hall crystal.

tion with a tripled unit cell corresponding to $\sqrt{3} \times \sqrt{3}$ moiré cells. Furthermore, we demonstrate that the QAHC arising from a $C = 2$ Chern band remains robust in a realistic model describing twisted double bilayer graphene (TDBG) [19, 55–58]. Finally, we scan the parameter space of experimental tuning knobs and predict the optimal twist angles and layer potentials to realize this phase in TDBG.

RESULTS

Ideal higher Chern bands. We consider ideal topological flat bands described by the chiral model of twisted multilayer graphene, which consists of two sheets of Bernal-stacked graphene, twisted by the magic angle and with artificially suppressed intra-sublattice tunneling between adjacent layers [53, 54]. The top and bottom sheets consists of m and n layers, respectively, and the model hosts a pair of exact flat bands with Chern number $C = m$ and $C = -n$, offering a perfect platform for investigating the emergence of QAHCs in higher Chern bands. These bands have an ideal quantum geometry, i.e. the Fubini-Study metric is proportional to the Berry curvature distribution in momentum space, implying that FCIs are in principle the exact ground states of short-range pseudopotential interactions [53]. Here, however, we are interested in electrons interacting via the long-range Coulomb potential.

The simplest way to describe an ideal Chern band with $C = 1$ is by taking $n = 1$ and $m = 1$, corresponding to the chiral model of twisted bilayer graphene. This model has been used

to emulate the lowest Landau-level physics with pseudopotential interactions [18], and e.g. to shed light on the particle-hole symmetry breaking which results in a Fermi liquid instead of FCI at $\nu = \frac{2}{3}$ [59]. Here we consider the Coulomb interaction and, after solving the many-body problem projected on the $C = 1$ band by ED (see Methods), we reveal a gapped phase characterized by three degenerate ground states appearing at the center-of-mass momenta expected for the $\nu = \frac{2}{3}$ FCI, cf. Fig. 1(a). A more thorough analysis shows that the Berry curvature of the three-fold degenerate many-body ground state is rather uniform [see Fig. 1(b)] and yields an average Chern number $C_{\text{avg}} = \frac{2}{3}$ for each ground state. The degeneracy and Chern number, as well as the hole-entanglement spectrum (see details in the Methods section and Supplemental Material [60], SM), indicate that the three ground states indeed correspond to the FCI phase. Aligned with this, the ground state structure factor $S(\mathbf{q})$ shown in Fig. 1(c) reveals a liquid-like feature, as no prominent peaks are observed in the moiré Brillouin zone (mBZ). The peaks outside the mBZ located at the Γ points of the outer shell ($\mathbf{q} = C_6^n \mathbf{G}_1$, i.e. six-fold rotation C_6^n of the reciprocal lattice vector \mathbf{G}_1) correspond to the first harmonics of the moiré potential. In fact, the real-space pair correlation function $G(\mathbf{r})$ follows the periodic modulation of the moiré lattice [Fig. 1(d)]. For a definition of $S(\mathbf{q})$ and $G(\mathbf{r})$ we refer the reader to the Methods section.

We now explore the nature of the $\nu = \frac{2}{3}$ state in the ideal higher Chern band with $C = 2$. Motivated by the recent experimental realization of topological crystals in twisted bilayer-trilayer graphene [48], we set $n = 2, m = 3$ to model this heterostructure in the chiral limit. After performing ED

on the $C = 2$ band with Coulomb interactions, we obtain a low-lying many-body energy spectrum that again exhibits a threefold degenerate ground state, see Fig. 1(e). However, by relating to the generalized exclusion rule in the thin-torus limit [61, 62], we rule out the competing order of a $\nu = \frac{2}{3}$ FCI phase, as then the three ground states should share the same momentum (the Γ point) for this specific tilted sample; see details in the SM [60]. Instead, the ground states are separated by the momentum \mathbf{K} (or \mathbf{K}'). Interestingly, in this case the Berry curvature yields an average many-body Chern number $C_{\text{avg}} = 1$ [Fig. 1(f)]. Based on previous works, the mismatch between the integer Chern number and the fractional filling factor ν suggests that the moiré translation symmetry is broken by the interactions. Indeed, a calculation of $S(\mathbf{q})$ confirms that the symmetry breaking is characterized by prominent peaks appearing at \mathbf{K} and \mathbf{K}' points [Fig. 1(g)], which implies a tripling of the unit cell. A more intuitive picture can be obtained in real space, where the pair correlation function $G(\mathbf{r})$ clearly follows a periodic crystal structure with a $\sqrt{3}a_m \times \sqrt{3}a_m$ unit cell (a_m is the moiré lattice parameter) that is three times larger than the moiré unit cell, cf. Fig. 1(h). We emphasize that these results are in agreement with the observation of a QAHC with integer-quantized Hall conductivity in twisted bilayer-trilayer graphene [48]. While we have considered this structure in the ideal chiral limit, we will demonstrate later that the QAHC remains robust in a realistic model.

For even higher ideal Chern bands $C > 2$, we have not observed any clearly gapped crystalline phase from the low-lying energy spectrum across various fillings. Instead Fermi-liquid states dictated by an effective dispersion related to the fluctuating quantum metric dominate the phase diagram [60, 63]. This is in line with results for another class of multilayer models with partially filled $C = n$ Chern bands which cannot exhibit gapped spectra as $n \rightarrow \infty$ [64]. We also note that the corresponding Wannier functions, bounded by the quantum metric, become extended for higher Chern number bands—making it more challenging to characterize any charge order [65]. On the other hand, the analogous situation in higher Landau levels with ideal quantum geometry $g_{\mathbf{k}} = (n + 1/2)\Omega_{\mathbf{k}}$, where the Hartree-Fock description of the fractional quantum Hall system becomes exact for large n [66, 67], in principle allows for charge ordered states (but not FCIs).

We note that additional observations show that these phases remain robust under variations in the number of layers in one sheet, e.g. m . This can already be seen from the fact that the single-particle quantum geometry of the target band remains unchanged and, consequently, considering interactions yields an identical behavior. Although this observation holds for the ideal chiral model, it prompts the question of to what extent it remains valid in realistic settings and whether it could aid future experimental investigations of such phases by simplifying the experimental setup, e.g. by considering bilayer-monolayer instead of bilayer-trilayer structures.

Twisted double bilayer graphene. After having determined

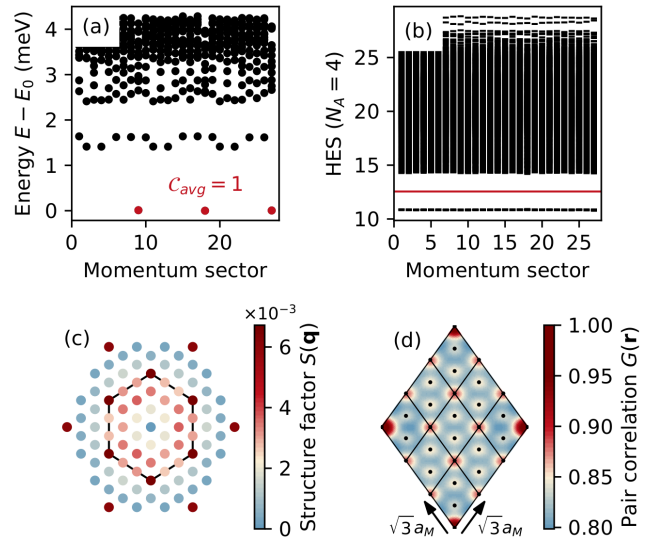


FIG. 2. Hall crystal at $\nu = \frac{2}{3}$ in realistic twisted double bilayer graphene with twist angle $\theta = 1.35^\circ$ and a vertical potential bias of $U = 60$ meV. (a) Many-body energy spectrum for $N_s = 27$ sites showing a threefold degenerate ground state with average many-body Chern number $C_{\text{avg}} = 1$. The parent single-particle band has a Chern number $C = 2$. (b) Hole entanglement spectrum, where the number of states below the red line is 378 and matches exactly the number of allowed quasi-hole excitations in a CDW. (c) Structure factor in the mBZ. (d) Pair-correlation function in the considered finite system.

that QAHCs are stable at $\nu = \frac{2}{3}$ filling of an ideal flat band with Chern number $C = 2$, we demonstrate the robustness of this phase in a realistic and experimentally accessible setting. In particular, we move away from the chiral limit and consider TDBG with finite intra-subband tunneling between adjacent layers $w_0 = 0.7w_1$, where w_1 is the inter-sublattice tunneling strength [19]. This model is characterized by a $C = 2$ conduction band that remains isolated for a relatively broad range of twist angles and layer potentials [55, 56] and which has been confirmed in experiments [68, 69]. At filling $\nu = 1/3$ the conduction band has been predicted to harbor an FCI phase beyond the Landau level paradigm [19].

We here consider filling $\nu = 2/3$ starting with twist angle $\theta = 1.35^\circ$ and layer potential $U = 60$ meV, at which the $C = 2$ Chern band is nearly flat and well isolated from neighboring bands [68]. Here, ED calculations with the same system size as above yield all the characteristic fingerprints of the QAHC phase: (i) a three-fold degenerate many-body ground state with an average Chern number $C_{\text{avg}} = 1$ [Fig. 2(a)]; (ii) a large gap in the HES, where the number of states below the gap is equal to the number of quasi-hole excitations in a CDW [Fig. 2(b)]; and (iii) a structure factor with pronounced \mathbf{K} -point peaks [Fig. 2(c)] resulting in a $\sqrt{3} \times \sqrt{3}$ CDW modulation [Fig. 2(d)]. In this realistic setting, though, the modulation arising from the moiré potential, which is visible in the strong $S(\mathbf{q})$ peaks at outer Γ points in Fig. 2(c), is quite significant. Nevertheless, we emphasize that even if the CDW

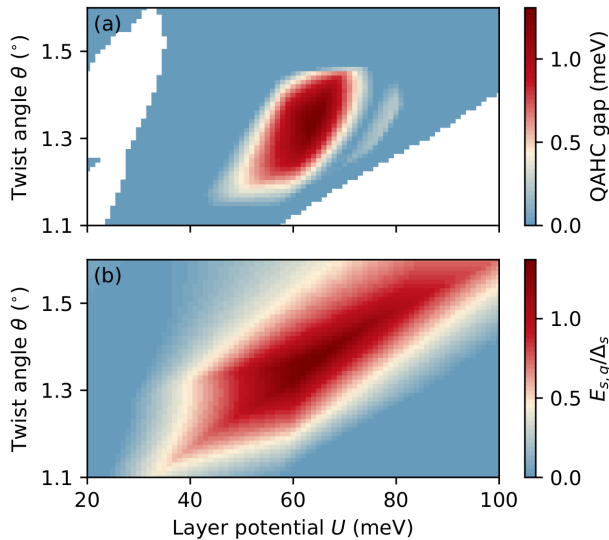


FIG. 3. Stability of the QAHC in the (U, θ) parameter space. (a) Energy gap in the many-body spectrum with respect to the QAHC ground states. The regions where the single-particle band is not isolated appear in white. The many-body spectra have been generated for a system of $N_s = 21$ sites with generating vectors $\mathbf{R}_1 = (4, -1)$, $\mathbf{R}_2 = (1, 5)$. (b) Ratio between the energy gap $E_{sp,g}$ and the bandwidth Δ_s of the single-particle band. The band has a Chern number $C = 2$ in the region where it is well isolated.

modulation is weak, the QAHC phase can still remain robust as long as the moiré translation symmetry is broken.

Next, we aim to explore the robustness of the QAHC in TDBG across the (U, θ) parameter space and find the optimal values at which this phase is most stable. To this end, we perform ED on the $C = 2$ conduction band across the range $U \in [20 \text{ meV}, 100 \text{ meV}]$ and $\theta \in [1.1^\circ, 1.6^\circ]$ and extract the energy gap in the many-body spectrum between the QAHC ground and excited states. As shown in Fig. 3(a), the QAHC remains stable with a gap $\sim 1 \text{ meV}$ for a relatively broad range of parameters, $U \in [50 \text{ meV}, 70 \text{ meV}]$ and $\theta \in [1.2^\circ, 1.45^\circ]$. A simple estimate relates these layer potentials to a displacement field $D = \epsilon U/d \in [0.18 \text{ V/nm}, 0.26 \text{ V/nm}]$, where we have taken $\epsilon = 5$ and $d = 4 \times 0.34 \text{ nm}$ [70, 71]. Importantly, the QAHC is stable in a parameter region where the single-particle band is well isolated and flat, i.e. where the ratio between the single-particle band gap $E_{sp,g}$ and the bandwidth Δ_{sp} is maximized, cf. Fig. 3(b). Note that the flatness condition in the odd-denominator filling $\nu = \frac{2}{3}$ seems to be in contrast with the recent observation that QAHCs at even-denominator filling require kinetic energy in order to be stable [40]. In addition, although there is an apparent closing and re-opening of the many-body gap at larger layer potentials which is reminiscent of a phase transition, our calculations of HES, Chern number, and structure factor indicate that the fringe with a finite gap emerging at $\approx 80 \text{ meV}$ still corresponds to the QAHC with $C_{\text{avg}} = 1$ and \mathbf{K} -point CDW modulation.

DISCUSSION

We have demonstrated the existence and robustness of QAHCs at $\nu = \frac{2}{3}$ filling of $C = 2$ Chern bands. First, we have shown that these phases emerge in ideal $C = 2$ bands, in particular in the chiral model of twisted bilayer-trilayer graphene—a heterostructure where experimental signatures of the QAHC have been recently observed. Unlike the previously QAHCs predicted by numerical works, which either were pinned at even-denominator filling factors or emerged in moiré-less systems, our results unveil topological crystals not only emerging at an odd-denominator filling factor $\nu = \frac{2}{3}$ but, moreover, originating from a higher Chern band with $C = 2$. This phase exhibits a \mathbf{K} -CDW modulation, characterized by a $\sqrt{3}a_m \times \sqrt{3}a_m$ unit cell, and supports a quantized Hall conductance of 1. Following the finding of QAHCs in ideal $C = 2$ bands, we have demonstrated that this phase remains robust in a realistic setting, concretely in TDBG. Importantly, we have predicted that the QAHC in this heterostructure remains stable in a relatively wide range of experimentally-accessible tuning parameters, namely for twist angles $\theta \in [1.2^\circ, 1.45^\circ]$ and layer potentials $U \in [50 \text{ meV}, 70 \text{ meV}]$.

From a theoretical perspective, the emergence of topological crystals in ideal flat bands establishes chiral twisted multilayer graphene as an excellent platform for further exploring novel properties of quantum anomalous Hall crystals and their connection to ideal quantum geometry. It has been long believed that the ideal quantum geometry favors the stabilization of FCIs against crystalline orders. However, the presence of QAHCs in this context challenges this general belief and therefore warrants further investigation. Additionally, as opposed to recent numerical studies on QAHCs in tMoTe₂ at even-denominator filling factors, where the kinetic energy plays a dominant role in driving the crystal phase [40], our study suggests a contrasting scenario: only interaction matters, as the band dispersion in the chiral model is exactly flat. Although twisted multilayer graphene differs substantially from moiré structures based on transition metal dichalcogenides, we believe our findings offer an alternative framework for understanding the fundamental nature of this new class of phases.

From a practical standpoint, our concrete prediction of a robust QAHC in TDBG considering experimentally accessible parameters offers a realistic and experimentally friendly guideline for discovering these phases. Given the strong connections of this realistic model to chiral models, our work could also be a starting point for searching more exotic topological phases of matter in moiré materials within higher Chern bands, thus going beyond the traditional paradigm of Landau level physics.

METHODS

To distinguish QAHCs and their competing orders, we employ brute-force ED to numerically extract both the low-

energy spectrum and ground state information at fractional fillings $\nu = N_e/N_s$. Here, N_e is the number of electrons and N_s is the number of moiré cells. The electron-electron interaction is projected onto the isolated and flat conduction band, and the resulting many-body Hamiltonian can be generally expressed as

$$H = \sum_{\mathbf{k}} E_{\mathbf{k}} c_{\mathbf{k}}^\dagger c_{\mathbf{k}} + \frac{1}{2} \sum_{\{\mathbf{k}_i\}} V_{\mathbf{k}_1 \mathbf{k}_2 \mathbf{k}_3 \mathbf{k}_4} c_{\mathbf{k}_1}^\dagger c_{\mathbf{k}_2}^\dagger c_{\mathbf{k}_3} c_{\mathbf{k}_4},$$

where $E_{\mathbf{k}}$ is the kinetic energy, $c_{\mathbf{k}}^\dagger$ is the electron creation operator with momentum \mathbf{k} , and $V_{\mathbf{k}_1 \mathbf{k}_2 \mathbf{k}_3 \mathbf{k}_4}$ is the Coulomb matrix element, which contains information of the single-particle wavefunction of the target band. We consider the Coulomb interaction $V(q) = \frac{1}{2A\epsilon|\mathbf{q}|}$ with the dielectric constant $\epsilon \approx 5$ that is typically considered in graphene systems [70].

To further clarify the nature of the phases, we calculate the structure factor and pair-correlation function averaged over the three-fold degenerate ground states, which provide insights on the crystalline or liquid character of the system. The structure factor is defined as $S(\mathbf{q}) = \frac{1}{N_e^2} \langle \rho(\mathbf{q})\rho(-\mathbf{q}) \rangle - \delta_{\mathbf{q},0}$, where $\rho(\mathbf{q})$ is the density operator projected onto the considered flat band. On the other hand, the real space pair-correlation function reads $G(\mathbf{r}) = \frac{1}{N_e^2} \langle n(\mathbf{r})n(\mathbf{0}) \rangle$, where $n(\mathbf{r})$ is the real-space density operator.

The fundamental nature of the many-body ground states can be accessed by the particle-cut entanglement spectrum (PES) [4, 72]. The PES, not to be confused with entanglement entropy, is obtained by dividing the many-body system into A and B subsystems consisting of N_A and $N_B = N_e - N_A$ particles, and then calculating the eigenvalues of $-\log \rho_A$, where $\rho_A = \text{tr}_B [\frac{1}{N_d} \sum_{i=1}^{N_d} |\Psi_i\rangle \langle \Psi_i|]$ is the reduced density matrix of A . Here, ρ_A carries crucial information about the quasi-hole excitations in the degenerate ground states $|\Psi_i\rangle$, which are characteristically distinct for FCIs and CDWs. In particular, a gap in the PES is expected, below which the number of states exactly matches the amount of quasi-hole excitations allowed by the specific quantum phase of the system. In this work, we have used the hole entanglement spectrum (HES), where N_A and $N_B = N_s - N_e - N_A$ now denote the number of holes [36]. The HES thus gives information about the quasi-particle excitations of the system.

Acknowledgements

We acknowledge useful discussions and related collaborations with Zhao Liu, Ahmed Abouelkomsan, Liang Fu, Aidan Reddy and Donna Sheng. This work was supported by the Swedish Research Council (2018-00313 and 2024-04567), the Knut and Alice Wallenberg Foundation (2018.0460 and 2023.0256) and the Göran Gustafsson Foundation for Research in Natural Sciences and Medicine. The computations were enabled by resources provided by the National Academic Infrastructure for Supercomputing in Sweden (NAIIS), partially funded by the Swedish Research Council through grant agreement no. 2022-06725; in addition, we utilized the

Sunrise HPC facility supported by the Technical Division at the Department of Physics, Stockholm University.

* raul.perea.causin@fysik.su.se

† hui.liu@fysik.su.se

‡ emil.bergholtz@fysik.su.se

- [1] E. Y. Andrei and A. H. MacDonald, Graphene bilayers with a twist, *Nature Materials* **19**, 1265–1275 (2020).
- [2] E. Y. Andrei, D. K. Efetov, P. Jarillo-Herrero, A. H. MacDonald, K. F. Mak, T. Senthil, E. Tutuc, A. Yazdani, and A. F. Young, The marvels of moiré materials, *Nature Reviews Materials* **6**, 201–206 (2021).
- [3] K. F. Mak and J. Shan, Semiconductor moiré materials, *Nature Nanotechnology* **17**, 686–695 (2022).
- [4] N. Regnault and B. A. Bernevig, Fractional Chern insulator, *Phys. Rev. X* **1**, 021014 (2011).
- [5] Z. Liu and E. J. Bergholtz, Recent developments in fractional Chern insulators, in *Encyclopedia of Condensed Matter Physics (Second Edition)*, edited by T. Chakraborty (Academic Press, Oxford, 2024) second edition ed., pp. 515–538.
- [6] E. J. Bergholtz and Z. Liu, Topological flat band models and fractional Chern insulators, *International Journal of Modern Physics B* **27**, 1330017 (2013).
- [7] S. A. Parameswaran, R. Roy, and S. L. Sondhi, Fractional quantum Hall physics in topological flat bands, *Comptes Rendus Physique* **14**, 816–839 (2013), topological insulators / Isolants topologiques.
- [8] A. Kol and N. Read, Fractional quantum Hall effect in a periodic potential, *Phys. Rev. B* **48**, 8890–8898 (1993).
- [9] E. Tang, J.-W. Mei, and X.-G. Wen, High-Temperature Fractional Quantum Hall States, *Physical Review Letters* **106**, 236802 (2011).
- [10] K. Sun, Z. Gu, H. Katsura, and S. Das Sarma, Nearly flatbands with nontrivial topology, *Phys. Rev. Lett.* **106**, 236803 (2011).
- [11] T. Neupert, L. Santos, C. Chamon, and C. Mudry, Fractional quantum Hall states at zero magnetic field, *Phys. Rev. Lett.* **106**, 236804 (2011).
- [12] D. Sheng, Z.-C. Gu, K. Sun, and L. Sheng, Fractional quantum Hall effect in the absence of Landau levels, *Nature Communications* **2**, 1–5 (2011).
- [13] G. Möller and N. R. Cooper, Composite fermion theory for bosonic quantum Hall states on lattices, *Phys. Rev. Lett.* **103**, 105303 (2009).
- [14] E. Kapit and E. Mueller, Exact parent Hamiltonian for the quantum Hall states in a lattice, *Phys. Rev. Lett.* **105**, 215303 (2010).
- [15] E. M. Spanton, A. A. Zibrov, H. Zhou, T. Taniguchi, K. Watanabe, M. P. Zaletel, and A. F. Young, Observation of fractional Chern insulators in a van der Waals heterostructure, *Science* **360**, 62–66 (2018).
- [16] A. Abouelkomsan, Z. Liu, and E. J. Bergholtz, Particle-hole duality, emergent Fermi liquids, and fractional Chern insulators in moiré flatbands, *Phys. Rev. Lett.* **124**, 106803 (2020).
- [17] C. Repellin and T. Senthil, Chern bands of twisted bilayer graphene: Fractional Chern insulators and spin phase transition, *Physical Review Research* **2**, 023238 (2020).
- [18] P. J. Ledwith, G. Tarnopolsky, E. Khalaf, and A. Vishwanath, Fractional Chern insulator states in twisted bilayer graphene: An analytical approach, *Phys. Rev. Research* **2**, 023237 (2020).
- [19] Z. Liu, A. Abouelkomsan, and E. J. Bergholtz, Gate-tunable fractional Chern insulators in twisted double bilayer graphene,

Phys. Rev. Lett. **126**, 026801 (2021).

[20] H. Li, U. Kumar, K. Sun, and S.-Z. Lin, Spontaneous fractional Chern insulators in transition metal dichalcogenide moiré superlattices, *Phys. Rev. Res.* **3**, L032070 (2021).

[21] T. Devakul, V. Crépel, Y. Zhang, and L. Fu, Magic in twisted transition metal dichalcogenide bilayers, *Nature Communications* **12**, 6730 (2021).

[22] P. Wilhelm, T. C. Lang, and A. M. Läuchli, Interplay of fractional Chern insulator and charge density wave phases in twisted bilayer graphene, *Phys. Rev. B* **103**, 125406 (2021).

[23] Y. Xie, A. T. Pierce, J. M. Park, D. E. Parker, E. Khalaf, P. Ledwith, Y. Cao, S. H. Lee, S. Chen, P. R. Forrester, K. Watanabe, T. Taniguchi, A. Vishwanath, P. Jarillo-Herrero, and A. Yacoby, Fractional Chern insulators in magic-angle twisted bilayer graphene, *Nature* **600**, 439–443 (2021).

[24] H. Park, J. Cai, E. Anderson, Y. Zhang, J. Zhu, X. Liu, C. Wang, W. Holtzmann, C. Hu, Z. Liu, T. Taniguchi, K. Watanabe, J.-H. Chu, T. Cao, L. Fu, W. Yao, C.-Z. Chang, D. Cobden, D. Xiao, and X. Xu, Observation of fractionally quantized anomalous Hall effect, *Nature* **622**, 74–79 (2023).

[25] J. Cai, E. Anderson, C. Wang, X. Zhang, X. Liu, W. Holtzmann, Y. Zhang, F. Fan, T. Taniguchi, K. Watanabe, Y. Ran, T. Cao, L. Fu, D. Xiao, W. Yao, and X. Xu, Signatures of fractional quantum anomalous Hall states in twisted MoTe₂, *Nature* **622**, 63–68 (2023).

[26] Y. Zeng, Z. Xia, K. Kang, J. Zhu, P. Knüppel, C. Vaswani, K. Watanabe, T. Taniguchi, K. F. Mak, and J. Shan, Thermodynamic evidence of fractional Chern insulator in moiré MoTe₂, *Nature* **622**, 69–73 (2023).

[27] Z. Lu, T. Han, Y. Yao, A. P. Reddy, J. Yang, J. Seo, K. Watanabe, T. Taniguchi, L. Fu, and L. Ju, Fractional quantum anomalous Hall effect in multilayer graphene, *Nature* **626**, 759–764 (2024).

[28] F. Xu, Z. Sun, T. Jia, C. Liu, C. Xu, C. Li, Y. Gu, K. Watanabe, T. Taniguchi, B. Tong, J. Jia, Z. Shi, S. Jiang, Y. Zhang, X. Liu, and T. Li, Observation of integer and fractional quantum anomalous Hall effects in twisted bilayer MoTe₂, *Phys. Rev. X* **13**, 031037 (2023).

[29] A. P. Reddy, N. Paul, A. Abouelkomsan, and L. Fu, Non-Abelian fractionalization in topological minibands, *Phys. Rev. Lett.* **133**, 166503 (2024).

[30] C. Wang, X.-W. Zhang, X. Liu, J. Wang, T. Cao, and D. Xiao, Higher Landau-level analogues and signatures of non-Abelian states in twisted bilayer MoTe₂ (2024), arXiv:2404.05697 [cond-mat.str-el].

[31] C. Xu, N. Mao, T. Zeng, and Y. Zhang, Multiple Chern bands in twisted MoTe₂ and possible non-Abelian states (2024), arXiv:2403.17003 [cond-mat.str-el].

[32] C.-E. Ahn, W. Lee, K. Yananose, Y. Kim, and G. Y. Cho, Non-Abelian fractional quantum anomalous Hall states and first Landau level physics of the second moiré band of twisted bilayer MoTe₂, *Phys. Rev. B* **110**, L161109 (2024).

[33] H. Liu, Z. Liu, and E. J. Bergholtz, Non-Abelian fractional Chern insulators and competing states in flat moiré bands (2024), arXiv:2405.08887 [cond-mat.str-el].

[34] F. Chen, W.-W. Luo, W. Zhu, and D. N. Sheng, Robust non-Abelian even-denominator fractional Chern insulator in twisted bilayer MoTe₂ (2024), arXiv:2405.08386 [cond-mat.str-el].

[35] Z. Liu, B. Mera, M. Fujimoto, T. Ozawa, and J. Wang, Theory of generalized Landau levels and implication for non-Abelian states (2024), arXiv:2405.14479 [cond-mat.mes-hall].

[36] H. Liu, R. Perea-Causin, and E. J. Bergholtz, Parafermions in moiré minibands (2024), arXiv:2406.08546 [cond-mat.str-el].

[37] K. Kang, B. Shen, Y. Qiu, Y. Zeng, Z. Xia, K. Watanabe, T. Taniguchi, J. Shan, and K. F. Mak, Evidence of the fractional quantum spin Hall effect in moiré MoTe₂, *Nature* **628**, 522–526 (2024).

[38] Z. Tešanović, F. m. c. Axel, and B. I. Halperin, “Hall crystal” versus Wigner crystal, *Phys. Rev. B* **39**, 8525–8551 (1989).

[39] X.-Y. Song, C.-M. Jian, L. Fu, and C. Xu, Intertwined fractional quantum anomalous Hall states and charge density waves, *Phys. Rev. B* **109**, 115116 (2024).

[40] D. N. Sheng, A. P. Reddy, A. Abouelkomsan, E. J. Bergholtz, and L. Fu, Quantum anomalous Hall crystal at fractional filling of moiré superlattices, *Phys. Rev. Lett.* **133**, 066601 (2024).

[41] J. Dong, T. Wang, T. Wang, T. Soejima, M. P. Zaletel, A. Vishwanath, and D. E. Parker, Anomalous Hall Crystals in Rhombohedral Multilayer Graphene. I. Interaction-Driven Chern Bands and Fractional Quantum Hall States at Zero Magnetic Field, *Phys. Rev. Lett.* **133**, 206503 (2024).

[42] T. Soejima, J. Dong, T. Wang, T. Wang, M. P. Zaletel, A. Vishwanath, and D. E. Parker, Anomalous Hall crystals in rhombohedral multilayer graphene. II. General mechanism and a minimal model, *Phys. Rev. B* **110**, 205124 (2024).

[43] Z. Dong, A. S. Patri, and T. Senthil, Stability of anomalous Hall crystals in multilayer rhombohedral graphene, *Phys. Rev. B* **110**, 205130 (2024).

[44] T. Tan and T. Devakul, Parent Berry curvature and the ideal anomalous Hall crystal, *Phys. Rev. X* **14**, 041040 (2024).

[45] N. Paul, G. Shavit, and L. Fu, Designing (higher) Hall crystals (2024), arXiv:2410.03888 [cond-mat.mes-hall].

[46] Y. H. Kwan, J. Yu, J. Herzog-Arbeitman, D. K. Efetov, N. Regnault, and B. A. Bernevig, Moiré fractional Chern insulators III: Hartree-Fock phase diagram, magic angle regime for Chern insulator states, the role of the moiré potential and Goldstone gaps in rhombohedral graphene superlattices (2023), arXiv:2312.11617 [cond-mat.str-el].

[47] Z. Lu, T. Han, Y. Yao, J. Yang, J. Seo, L. Shi, S. Ye, K. Watanabe, T. Taniguchi, and L. Ju, Extended quantum anomalous Hall states in graphene/hBN moiré superlattices (2024), arXiv:2408.10203 [cond-mat.mes-hall].

[48] R. Su, D. Waters, B. Zhou, K. Watanabe, T. Taniguchi, Y.-H. Zhang, M. Yankowitz, and J. Folk, Topological electronic crystals in twisted bilayer-trilayer graphene (2024), arXiv:2406.17766 [cond-mat.mes-hall].

[49] D. Waters, A. Okounkova, R. Su, B. Zhou, J. Yao, K. Watanabe, T. Taniguchi, X. Xu, Y.-H. Zhang, J. Folk, and M. Yankowitz, Interplay of electronic crystals with integer and fractional Chern insulators in moiré pentalayer graphene (2024), arXiv:2408.10133 [cond-mat.mes-hall].

[50] Z. Liu, E. J. Bergholtz, H. Fan, and A. M. Läuchli, Fractional Chern insulators in topological flat bands with higher Chern number, *Phys. Rev. Lett.* **109**, 186805 (2012).

[51] A. Sterdyniak, C. Repellin, B. A. Bernevig, and N. Regnault, Series of Abelian and non-Abelian states in $C > 1$ fractional Chern insulators, *Phys. Rev. B* **87**, 205137 (2013).

[52] J. Behrmann, Z. Liu, and E. J. Bergholtz, Model fractional Chern insulators, *Phys. Rev. Lett.* **116**, 216802 (2016).

[53] J. Wang and Z. Liu, Hierarchy of ideal flatbands in chiral twisted multilayer graphene models, *Phys. Rev. Lett.* **128**, 176403 (2022).

[54] P. J. Ledwith, A. Vishwanath, and E. Khalaf, Family of ideal Chern flatbands with arbitrary Chern number in chiral twisted graphene multilayers, *Phys. Rev. Lett.* **128**, 176404 (2022).

[55] J. Y. Lee, E. Khalaf, S. Liu, X. Liu, Z. Hao, P. Kim, and A. Vishwanath, Theory of correlated insulating behaviour and spin-triplet superconductivity in twisted double bilayer graphene, *Nature Communications* **10**, 5333 (2019).

[56] N. R. Chebrolu, B. L. Chittari, and J. Jung, Flat bands in twisted double bilayer graphene, *Phys. Rev. B* **99**, 235417 (2019).

[57] M. Koshino, Band structure and topological properties of twisted double bilayer graphene, *Phys. Rev. B* **99**, 235406 (2019).

[58] F. Haddadi, Q. Wu, A. J. Kruchkov, and O. V. Yazyev, Moiré flat bands in twisted double bilayer graphene, *Nano Letters* **20**, 2410–2415 (2020).

[59] H. Liu, K. Yang, A. Abouelkomsan, Z. Liu, and E. J. Bergholtz, Broken symmetry in ideal Chern bands (2024), arXiv:2402.04303 [cond-mat.str-el].

[60] See supplemental material for additional details including the Berry curvature of the single-particle bands, hole entanglement spectrum for the ideal $C = 1, C = 2$ Chern bands, and exact-diagonalization results for the ideal $C = 3$ band..

[61] E. J. Bergholtz and A. Karlhede, Quantum Hall system in Tao-Thouless limit, *Phys. Rev. B* **77**, 155308 (2008).

[62] B. A. Bernevig and N. Regnault, Emergent many-body translational symmetries of Abelian and non-Abelian fractionally filled topological insulators, *Phys. Rev. B* **85**, 075128 (2012).

[63] A. Abouelkomsan, K. Yang, and E. J. Bergholtz, Quantum metric induced phases in moiré materials, *Phys. Rev. Res.* **5**, L012015 (2023).

[64] E. J. Bergholtz, Z. Liu, M. Trescher, R. Moessner, and M. Udagawa, Topology and interactions in a frustrated slab: Tuning from Weyl semimetals to $C > 1$ fractional Chern insulators, *Phys. Rev. Lett.* **114**, 016806 (2015).

[65] A. P. Reddy, D. N. Sheng, A. Abouelkomsan, E. J. Bergholtz, and L. Fu, Anti-topological crystal and non-Abelian liquid in twisted semiconductor bilayers (2024), arXiv:2411.19898 [cond-mat.mes-hall].

[66] R. Moessner and J. T. Chalker, Exact results for interacting electrons in high Landau levels, *Phys. Rev. B* **54**, 5006–5015 (1996).

[67] D. Yoshioka, Higher Landau levels, in *The Quantum Hall Effect* (Springer Berlin Heidelberg, Berlin, Heidelberg, 2002) pp. 173–187.

[68] X. Liu, Z. Hao, E. Khalaf, J. Y. Lee, Y. Ronen, H. Yoo, D. Haei Najafabadi, K. Watanabe, T. Taniguchi, A. Vishwanath, and P. Kim, Tunable spin-polarized correlated states in twisted double bilayer graphene, *Nature* **583**, 221–225 (2020).

[69] Y. Wang, J. Herzog-Arbeitman, G. W. Burg, J. Zhu, K. Watanabe, T. Taniguchi, A. H. MacDonald, B. A. Bernevig, and E. Tutuc, Bulk and edge properties of twisted double bilayer graphene, *Nature Physics* **18**, 48–53 (2022).

[70] F. Wu, T. Lovorn, E. Tutuc, and A. H. MacDonald, Hubbard model physics in transition metal dichalcogenide moiré bands, *Phys. Rev. Lett.* **121**, 026402 (2018).

[71] Z. H. Ni, H. M. Wang, J. Kasim, H. M. Fan, T. Yu, Y. H. Wu, Y. P. Feng, and Z. X. Shen, Graphene thickness determination using reflection and contrast spectroscopy, *Nano Letters* **7**, 2758–2763 (2007).

[72] A. Sterdyniak, N. Regnault, and B. A. Bernevig, Extracting Excitations from Model State Entanglement, *Physical Review Letters* **106**, 100405 (2011).